Journal of Biomedical Optics

SPIEDigitalLibrary.org/jbo

Perfusion assessment in rat spinal cord tissue using photoplethysmography and laser Doppler flux measurements

Justin P. Phillips
Vincent Cibert-Goton
Richard M. Langford
Peter J. Shortland

SPIE

Perfusion assessment in rat spinal cord tissue using photoplethysmography and laser Doppler flux measurements

Justin P. Phillips,[a] Vincent Cibert-Goton,[b] Richard M. Langford,[c] and Peter J. Shortland[b]
[a]City University London, School of Engineering and Mathematical Sciences, Northampton Square, London, United Kingdom
[b]Queen Mary University of London, Centre for Neuroscience and Trauma, Blizard Institute, Barts and the London School of Medicine and Dentistry, London, United Kingdom
[c]Queen Mary University of London, Pain and Anaesthesia Research Centre London, William Harvey Research Institute, Barts and the London School of Medicine and Dentistry, London, United Kingdom

Abstract. Animal models are widely used to investigate the pathological mechanisms of spinal cord injury (SCI), most commonly in rats. It is well known that compromised blood flow caused by mechanical disruption of the vasculature can produce irreversible damage and cell death in hypoperfused tissue regions and spinal cord tissue is particularly susceptible to such damage. A fiberoptic photoplethysmography (PPG) probe and instrumentation system were used to investigate the practical considerations of making measurements from rat spinal cord and to assess its suitability for use in SCI models. Experiments to assess the regional perfusion of exposed spinal cord in anesthetized adult rats using both PPG and laser Doppler flowmetry (LDF) were performed. It was found that signals could be obtained reliably from all subjects, although considerable intersite and intersubject variability was seen in the PPG signal amplitude compared to LDF. We present results from 30 measurements in five subjects, the two methods are compared, and practical application to SCI animal models is discussed. [DOI: 10.1117/1.JBO.18.3.037005]

Keywords: spinal cord injury; fiberoptic; photoplethysmography; laser Doppler; perfusion; ischemia.

Paper 12742R received Nov. 16, 2012; revised manuscript received Jan. 21, 2013; accepted for publication Feb. 18, 2013; published online Mar. 11, 2013.

1 Introduction

The mechanisms of tissue damage during and after spinal cord injury (SCI) are complex and incompletely understood.[1,2] Trauma causing SCI is classed as primary injury and can produce laceration, stretching, or compression of the delicate nervous tissue of the spinal cord, including avulsion of the spinal roots. Primary injury can give rise to hemorrhage, edema, and other physiologic responses, which can lead to local ischemia-related injury (known as secondary injury) in the minutes, hours, and days after the initial impact[3] via disruption of the blood spinal cord barrier.[4] Such secondary injury can cause serious permanent loss of function; however, appropriate and rapid hospital treatment can potentially minimize these effects.[1,5]

Several animal models have been developed to investigate various SCI mechanisms, most commonly in adult rats. Such models apply mechanical force to the spinal cord of anesthetized animals, including compression,[6] spinal root avulsion,[7,8] laceration,[9] etc. These models allow the effects of mechanical injury on neuronal damage and subsequent recovery to be studied under controlled conditions. Secondary injury resulting from disruption of the blood supply, either by laceration, occlusion, or other deformation of blood vessels, can lead to prolonged ischemia,[10,11] even after very mild trauma.[12] The tissue of the spinal cord, like all central nervous system tissue, is extremely sensitive to hypoxia or anoxia resulting from hypoperfusion, and irreversible ischemic injury can result within a very short time.[13] Quantification of ischemia resulting from SCI is traditionally performed by postmortem examination of the distribution and extent of cell death in histological specimens.[10] This process is time-consuming and often requires large numbers of specimens to obtain reliable results.

Several techniques have been used to quantify perfusion in the spinal cord before and after injury. Laser Doppler flowmetry (LDF),[14] the most widely used methodology, is used in several animal and human studies[15–17] to evaluate infarction and compromised blood flow in the spinal cord so that the contribution of ischemia to the total amount of secondary injury may be understood better. More specifically, the technique has been used to study the effects of hypothermia[18] and ischemic preconditioning[19] in limiting secondary injury in rat spinal cord tissue. Although laser Doppler is undoubtedly a useful technique, especially for comparative studies, its limitations should be considered. Specifically, LDF does not measure flow directly; rather it measures "flux"; i.e., the product of velocity and erythrocyte concentration in the proximity of the probe. The flux is nonlinear and cannot be calibrated with absolute flow. Instead, arbitrary units are used.[20] Another disadvantage is sensitivity to movement artifact.[21] Despite these limitations, LDF was used in the present study as a reference, as its use in similar areas of research is well established.

Several methods of direct measurement of cord blood flow have been demonstrated, including injection of radioactive microspheres[22] and hydrogen clearance;[23] however, neither technique is able to provide continuous measurement.

Address all correspondence to: J. P. Phillips, City University London, School of Engineering and Mathematical Sciences, Northampton Square, London, United Kingdom. Tel: +44 (0)207 040 8920; Fax: +44 (0)20 7040 8568; E-mail: Justin.Phillips.1@city.ac.uk

0091-3286/2013/$25.00

Computed tomography (CT) has also been used to measure spinal cord blood flow,[24] but the cost of CT scanners is prohibitive to most centers.

Photoplethysmography (PPG)[25] is the recording of blood volume changes by measurement of changes in light absorption. PPG is utilized in pulse oximetry, whereby a probe attached to the finger records a PPG signal from the arterioles in the subcutaneous tissue. The PPG signal recorded by the probe shows periodic changes in intensity, with each cardiac cycle appearing as a peak. Systolic distension of the arterioles causes increased absorption and a subsequent reduction in the detected intensity of the light reaching the photodetector in the pulse oximeter probe. Conversely, relaxation of the vessels during diastole causes an increase in detected intensity. The amplitude of the PPG signal indicates the availability of blood supply to the tissue. Many commercial pulse oximeters describe this variable as the "perfusion index" of the tissue.[26]

PPG has been applied in a limited context to nervous tissue monitoring,[27] but the use of the technique for monitoring perfusion in SCI models has not been widely investigated. This is probably due to the lack of availability of a commercial monitor; however, a small pilot study has been completed,[28] which demonstrated that acute SCI produced reduced PPG amplitude signals that recovered after the compression was removed. It should be noted that, like LDF, PPG does not provide direct measurement of blood flow.[29] PPG measurements could be applied to comparative studies, with or without LDF measurement, to provide a more comprehensive assessment of local perfusion status before trauma, after trauma, or both.

As a prelude to using this methodology to investigate the consequences of trauma on the spinal cord vascular response, an experimental protocol was established to assess regional perfusion of exposed spinal cord in anesthetized, naïve adult rats using both PPG and LDF. Here, we present results from 30 measurements in naïve subjects; sample signals are shown, the two modalities are statistically compared, and a discussion of the practical application of PPG to SCI animal models is included.

2 Materials and Methods

The optical fiber oximetry system comprises a probe and instrumentation connected to a data acquisition system, to which a commercial laser Doppler flowmeter is also connected. A block diagram of the system is shown in Fig. 1.

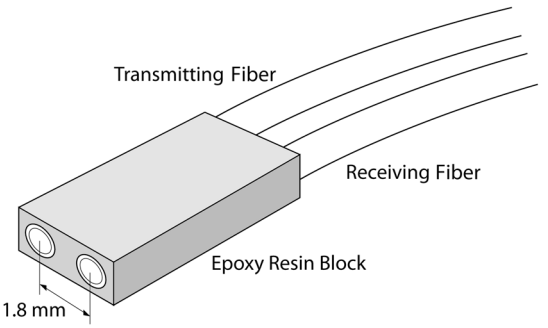

Fig. 2 Fiberoptic PPG probe.

2.1 *PPG Probe*

The PPG probe (Fig. 2) is fabricated from two silica glass optical fibers (SpecTran Speciality Optics, Avon, Connecticut), of 200-μm core diameter, surrounded by cladding and primary buffer; the overall diameter for each fiber of approximately 0.9 mm. The fibers are ordinarily coated in a protective polyvinyl chloride (PVC) sleeve; however, this was stripped off at the distal end, exposing a 7.5-cm length of fiber. The distal tips of each fiber were polished flat, and the proximal ends were terminated with small microwave adapter (SMA) connectors. The fibers are arranged in a parallel configuration with the distal ends separated by a distance of 1.4 mm (measured between the axes of the fibers) and held in position by an epoxy molding. One fiber transmits light to the tissue, while the second fiber transmits a portion of the backscattered light away from the tissue, enabling measurement of the backscattered intensity.

The transmitting fiber is connected to the two light sources via a bifurcated optical fiber assembly (Ocean Optics Inc., Dunedin, Florida). The detecting fiber is coupled directly to the photodetector. The footprint of the probe (i.e., the area of contact with the tissue) measures approximately 3.2 by 1.3 mm.

2.2 *Instrumentation*

The instrumentation is housed in a screened metal case containing several light sources [SMA mounted red (660-nm) and infrared (850-nm) LEDs (the Optoelectronic Manufacturing Corporation Ltd., Redruth, United Kingdom)]; a photodetector [an SMA mounted PIN photodiode (The Optoelectronic

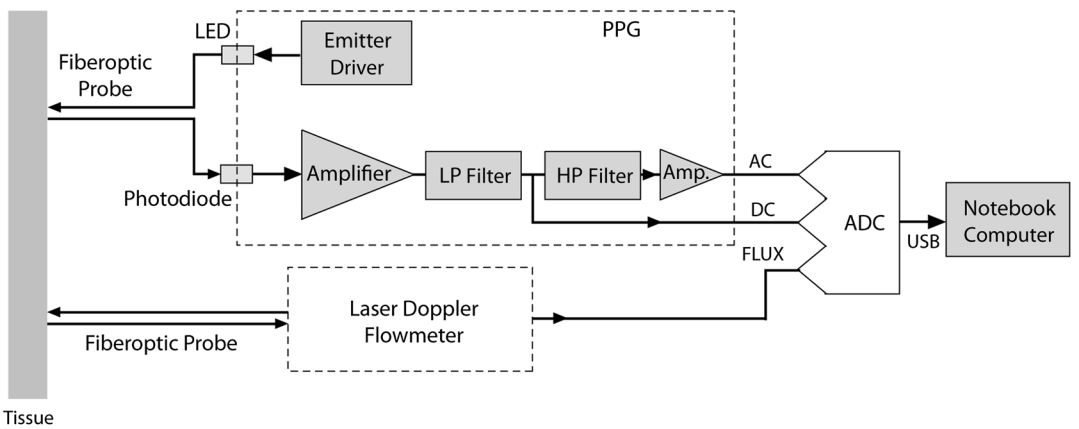

Fig. 1 Block diagram of a PPG system.

Manufacturing Corporation Ltd.)]; a power supply (2×12 V lead-acid batteries); and a circuit comprising two switchable regulated current sources connected to the LEDs and a 110-dB differential transimpedance amplifier, a demultiplexing circuit, and filters (to attenuate noise and to separate the AC and DC components of the signal) connected to the photodiode. The ac signal was band-pass-filtered with a pass-band ranging from 1 Hz to 19.4 Hz to remove the zero-frequency component and high-frequency interference. The DC signal was low-pass-filtered with a cutoff frequency of 19.4 Hz, to remove high-frequency interference while preserving any physiological artifacts. The pass-bands differ from those typically used in pulse oximeters designed for human use due to the higher heart rates recorded from small animals compared to humans. The AC signal was also passed through a final 40-dB amplifier stage.

2.3 *Data Acquisition System*

The LEDs are controlled by the digital multiplexing signal from a 16-bit PCMCIA data acquisition card (DAQCard-AI-16XE-50, National Instruments Inc., Austin, Texas), which performs the function of an analog-digital converter (ADC). The data acquisition card installed in a Sony VAIO PCG-Z600HEK notebook computer running a LabVIEW (National Instruments) virtual instrument (VI). The VI allows the user to control the multiplexing frequency of the light sources and the sampling frequency. The VI reads each of the four PPG signals (red AC, red DC, infrared AC, and infrared DC) at a rate of 200 samples per second. Digital filtering is applied to the DC signals (low pass filter, cutoff frequency 2.4 Hz). The VI also displays the PPG waveform and records the signals in a spreadsheet file.

2.4 *Laser Doppler System*

A moor VMS-LDF laser Doppler monitor (Moor Instruments Ltd., Axminster, United Kingdom) was used for the flux measurements. A VP3 cylindrical needle probe (Moor Instruments Ltd.) with a length of 40 mm, external diameter of 1.5 mm, and interfiber separation of 0.5 mm was used with the monitor. The fiber core diameter is approximately 125 μm. Simultaneous PPG and LDF measurements could not be made for two reasons: the footprints of the probes were not sufficiently small to allow both probes to be placed on the short length of cord under investigation, and earlier attempts showed that light from the laser was found to be picked up by the PPG probe saturation of the photodiode amplifier. Instead, PPG measurements were followed immediately by the LDF measurements.

3 Measurement Methods

A total of 30 measurements were taken from five adult male Wistar rats (Charles River Laboratories International, Wilmington, Massachusetts), from eight to nine weeks old and weighing approximately 12.35 ounces (350 g) at the time of surgery. All experiments were performed according to the UK Scientific Procedures Act (1986).

3.1 *Surgical Procedures and Measurements*

Each animal was deeply anesthetized in a fume box with a mixture of 4% Isofluorane in oxygen at a flow rate of 1.5 L per min. Throughout the procedure, anesthesia was maintained using 1.5% to 2% Isofluorane with oxygen at the same rate and delivered through a nosepiece. After incision of the skin and muscle overlying the lumbar spinal column under a surgical microscope (Carl, Germany), a bilateral laminectomy was performed aseptically at three successive vertebral levels (Thoracic T12; Lumbar L1 and L2) in order to expose the dorsal aspect of the spinal cord. This procedure allowed easy laser Doppler or PPG probe access to the three corresponding lumbar spinal levels (Lumbar L4, L5, and L6), while leaving the dura and arachnoid mater undisturbed.

Anesthetized animals were not given neuromuscular blocking drugs or artificial ventilation. Electrical artifacts related to breathing and heartbeat (i.e., ECG) were filtered during postrecording analysis. Rectal temperature of the animal was kept around 36°C with a controlled homeothermic blanket. The animal was placed in a frame and held prone with clamps placed on the T11 and L3 spinal vertebrae. The probe (PPG or Doppler) was subsequently placed just above the cord dorsum surface at the exposed spinal segments using a micromanipulator. Measurements were recorded just medial to the root entry zone (REZ) at three different levels along the rostro-caudal axis (L4, 5, and 6) and on both the left and right sides of the cord (referred to as positions A, B, C, A', B', C' in the results; see Fig. 3). PPG signals were recorded at each position for 2 min (12 min total measurement time), followed immediately by LDF signals recorded at each position in the same sequence (A, B, C, etc.). Thus, a 12-min delay separated PPG and LDF measurements made at each position. The spinal cord surface was kept humidified throughout the experiment with 0.9% saline heated to 36°C. At the end of the experiment, animals were euthanized with pentobarbital (200 mg/ml solution, Nembutal, injected intraperitoneally at 1 g/kg).

4 Signal Processing

The raw signals (PPG and Doppler) recorded during each 2-min sample period were divided into four epochs of 30 s duration.

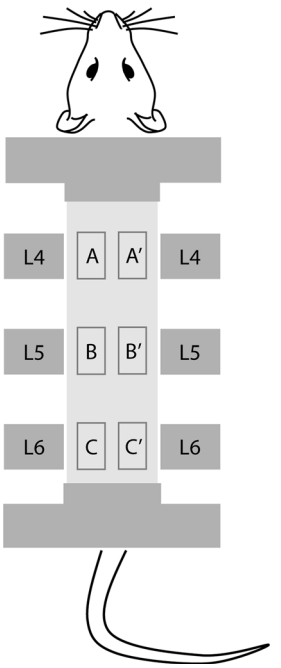

Fig. 3 Schematic diagram showing the position of the six monitoring sites on the surface of the L4–6 spinal cord used in the experiments.

The first and last epochs were discarded and the second and third epochs combined to produce a one-minute sample of each measurement. This ensured that artifacts caused by the movement of the probe relative to the tissue or by settling of the measurement system were minimized.

An amplitude spectrum was obtained from a discrete Fourier transform (DFT) using a Hamming window. The amplitude spectrum was normalized by dividing the raw signal by the dc (0 Hz) signal. Normalization compensates for various effects, such as variations in light source intensity and the spectral sensitivity of the photodiode. Also, the PPG AC: DC ratio is used in the algorithms to estimate arterial oxygen saturation in pulse oximeters. The amplitude spectrum of each Doppler signal was also produced, from which the amplitude of the Doppler signal was calculated over different frequency ranges.

To allow quantitative comparison of the PPG and LDF signals, several variables were derived from the amplitude spectra of the raw signals: the normalized amplitudes of the PPG signal were calculated from the height of the spectral peak over the spectral range $f_c \pm 0.015$ Hz, where f_c is the cardiac frequency at the time of recording, divided by the dc signal. For all measurements, the cardiac frequency was determined by identifying the spectral maximum occurring above 3 Hz. The laser Doppler signal amplitude was calculated over a very low frequency range: 0 to 0.03 Hz ("steady flow Doppler"), in recognition of the fact that unlike PPG, the Doppler signal is not completely pulsatile but contains a significant "steady flow" component. The amplitude was also calculated over the range $f_c \pm 0.015$ Hz (pulsatile Doppler) to compare the pulsatile flow measured at each site with the corresponding PPG amplitude.

5 Results

Figure 4 shows a 10-s sample of the low-pass-filtered (DC) infrared PPG signal recorded at one measurement site (A', Subject #1) plotted against time. Respiratory and cardiac effects can be observed in the recorded trace. There is a large periodic low frequency (<1 Hz) component caused by spontaneous respiration. In addition, the cardiac pulse component may also be clearly seen.

Figure 5 shows the amplitude spectrum of the low-pass-filtered (DC) PPG signal from the same site, subject, and sample period obtained from a DFT. The dominant peak at around 0.7 Hz is caused by respiratory movement, while the peak at 5.3 Hz results from the cardiac pulse. The numerous peaks between these peaks are harmonics of the respiratory peak.

Figure 6 shows the time-domain laser Doppler signal acquired from the same measurement site and subject as Figs. 4 and 5. The signal shows some variation with time; however, the periodicity seen in the PPG signal is not present.

Figure 7 shows the amplitude spectrum of the LDF signal from the same site, subject, and sample period. Small respiratory and cardiac peaks are visible at 0.7 and 4.66 Hz, respectively; however, they are much less prominent than those in Fig. 5.

6 Comparison between PPG and LDF

Tables 1–3 show the PPG amplitude and magnitude of the Doppler flux measurements at the two frequency ranges described in methods together with the mean amplitude, standard deviation (SD) from the mean amplitude, and coefficient of variability (CV) for all sites and for all subjects. The correlation between the PPG and the two Doppler flux measurements was evaluated by calculating the coefficient of determination between PPG and each of the two LDF values. It can be seen that the amplitudes of the PPG signals are small: 0.0005 to 0.0008; i.e., 0.05% to 0.08% of the total detected radiation intensity. This optical pulse is approximately one-tenth the magnitude of typical finger PPG signals recorded by a pulse oximeter probe in a human subject with good peripheral perfusion.[25]

The repeatability of the measurements may be assessed by considering the CV for measurements within each subject (at different measurement sites) and between subjects. Both the Doppler and PPG amplitudes were seen to vary considerably between measurement sites in most subjects. In fact, the Doppler "steady flow" flux is more repeatable than that of PPG, while the Doppler "pulsatile" flux is more variable than that of PPG.

7 Discussion

The amount of intersite variability in both PPG amplitude and Doppler flux is surprising, considering that there is no tangible difference between measurement sites, except possibly the distribution and/or density of blood vessels. Comparing different subjects (at the same measurement site) also shows that "steady flow" Doppler is more repeatable, while "pulsatile" Doppler is more variable.

Between-subject differences could be explained by global hemodynamic variables, such as blood pressure, cardiac output, and/or depth of anesthesia, although we are forced to speculate

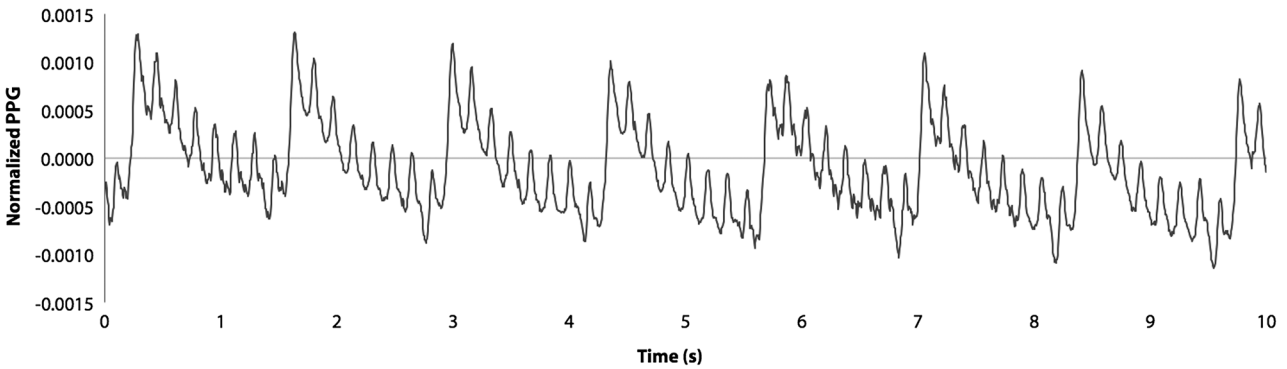

Fig. 4 Graph showing a 10-s sample of the low-pass-filtered infrared PPG signal (site A', Subject #1).

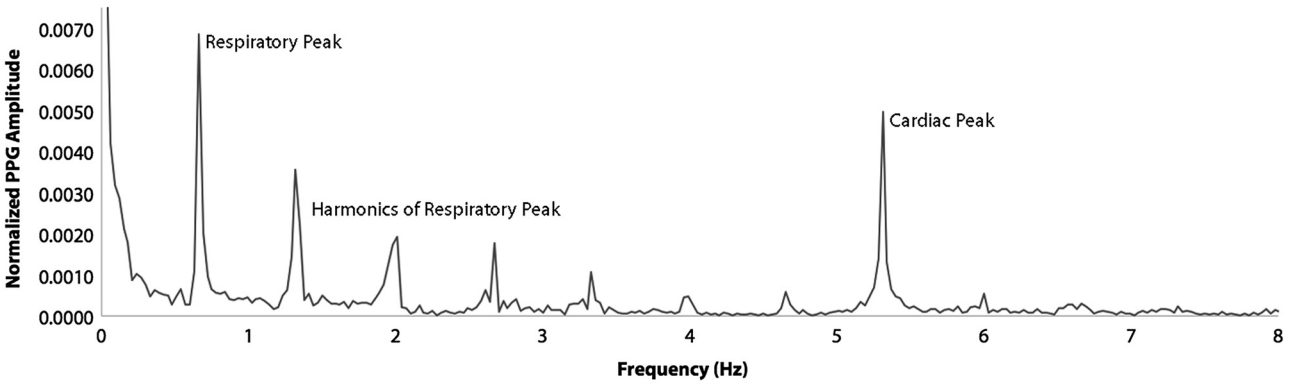

Fig. 5 Amplitude spectrum of the infrared PPG signal (site A′, Subject #1) obtained from a DFT showing cardiac peak and respiratory peaks with associated harmonics.

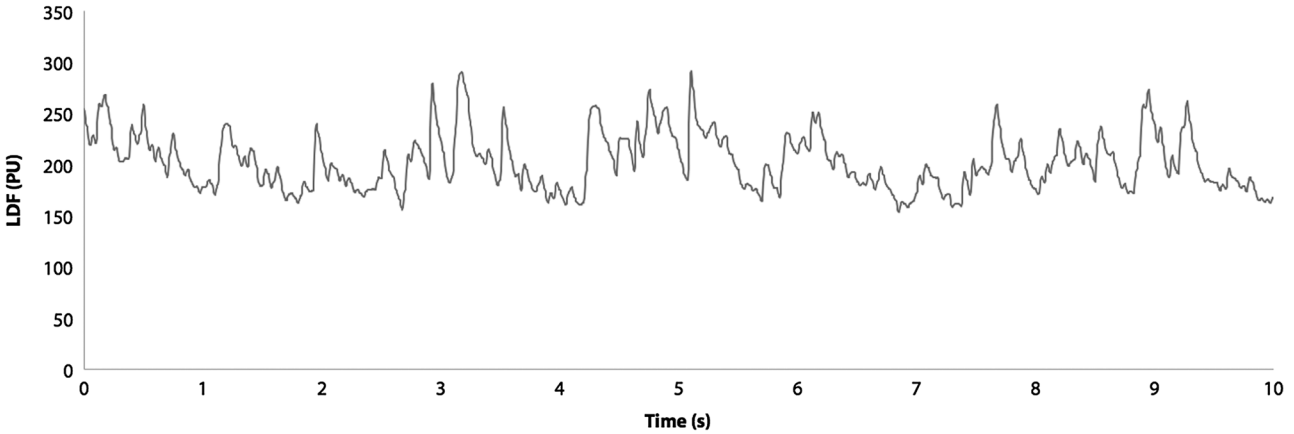

Fig. 6 A 10-s sample of the LDF signal in arbitrary perfusion units (site A′, Subject #1).

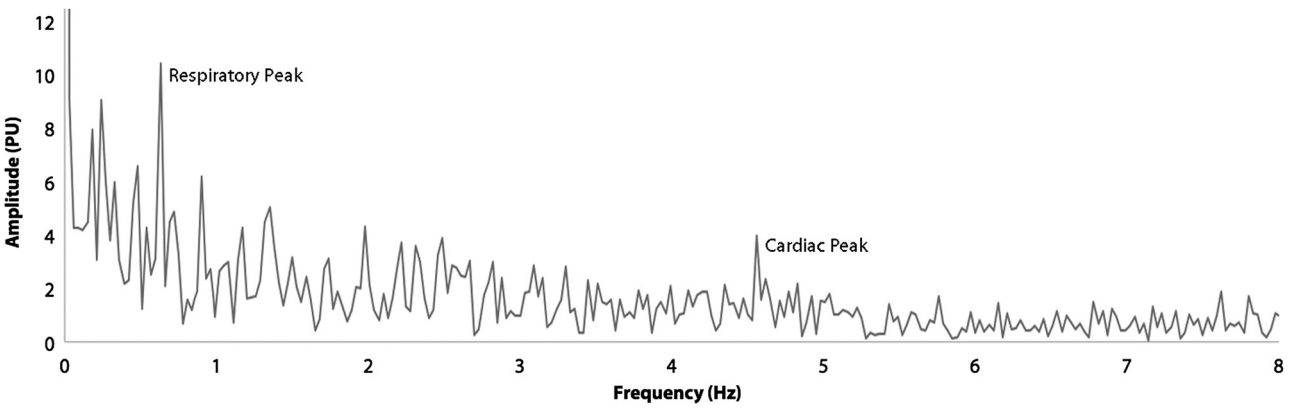

Fig. 7 Amplitude spectrum of the LDF signal in arbitrary perfusion units (site A′, Subject #1) showing respiratory and cardiac peaks.

regarding this point because these variables were not measured. Some variability may undoubtedly be caused by simply removing and repositioning the probe over a measurement site. Microscopic differences in position and/or application pressure almost certainly would cause differences in reported values. During the measurements, every care was taken to place the probe so the tip was in light contact with the tissue, exerting no excess pressure. However, without a sensitive pressure sensor at the probe tip, absolute consistency is impossible to attain. Note that although simultaneous PPG signals were recorded using infrared (850-nm) and red (660-nm) multiplexed light sources, only the infrared signals were analyzed. This was because the red signals, although of good quality, were smaller in amplitude than the infrared signals and give no additional information regarding tissue perfusion.

The correlation between PPG amplitude and both laser Doppler flux (LDF) values for all measurements (regardless of site or subject) was also investigated. The coefficient of

Table 1. Mean normalized PPG amplitudes calculated at cardiac frequency f_c, showing inter-site CV (bottom row), and inter-subject CV (far right column).

	PPG: normalized amplitudes						
Site\subject	1	2	3	4	5	Mean	CV (%)
A	0.000526	0.000440	0.000171	0.000722	0.000515	0.000475	41.9
B	0.000422	0.000324	0.000453	0.000722	0.000424	0.000469	31.9
C	0.000756	0.000864	0.000704	0.000848	0.000331	0.000701	30.9
A′	0.000952	0.000467	0.000627	0.00101	0.000230	0.000658	50.0
B′	0.000573	0.000780	0.000333	0.00119	0.000482	0.000673	49.6
C′	0.000938	0.000773	0.000670	0.00133	0.000308	0.000803	46.4
Mean	0.000695	0.000608	0.000493	0.000971	0.000382		
CV (%)	32.0	36.9	43.0	26.0	28.8		

Table 2. Mean Doppler flux (low-pass filtered), showing inter-site CV (bottom row), and inter-subject CV (far right column).

	"Steady flow" LDF: 0.0–0.03 Hz (PU)						
Site\subject	1	2	3	4	5	Mean	CV (%)
A	210	233	270	218	156	217	19.0
B	315	162	241	203	237	232	24.4
C	238	325	341	145	427	295	36.4
A′	155	273	296	246	294	253	23.1
B′	171	298	341	173	142	225	39.3
C′	218	313	218	211	131	218	29.6
Mean	218	267	285	199	231		
CV (%)	26.0	22.9	18.0	17.8	49.7		

Table 3. Mean normalized PPG amplitudes calculated at cardiac frequency f_c, showing inter-site CV (bottom row), and inter-subject CV (far right column).

	"Pulsatile" LDF: $f_c \pm 0.015$ Hz (PU)						
Site\subject	1	2	3	4	5	Mean	CV (%)
A	7.76	11.3	6.39	5.21	1.98	6.53	52.4
B	15.10	3.54	3.00	5.21	6.70	6.71	73.2
C	5.96	3.96	8.37	4.56	4.57	5.48	32.3
A′	4.33	5.29	5.60	2.46	8.50	5.24	42.0
B′	11.20	5.53	15.0	2.97	2.77	7.49	72.1
C′	9.44	2.65	5.31	5.17	5.36	5.59	43.6
Mean	8.97	5.38	7.28	4.26	4.98		
CV (%)	43.2	57.6	57.2	29.0	48.8		

determination (r^2) between PPG and "steady flow" Doppler was small ($r^2 = 0.043$). PPG and pulsatile flux showed a slightly stronger correlation ($r^2 = 0.102$). At first, this may seem surprising, as both PPG and LDF are considered surrogate measurements of the same quantity: blood flow. However, each technique is not only based on a different measurement principle but also measures two different physical effects. While LDF is related to blood cell velocity, PPG is related to arteriolar volume. Indeed, in the case of complete venous occlusion of a limb, it is possible for a pulse to be discerned and a pulse oximeter pleth wave to be seen on a monitor, despite the complete absence of blood flow. Despite these fundamental differences, PPG and LDF may be considered as two different aspects of perfusion that can give information about flow and oxygenation levels.

8 Conclusions

The authors consider that PPG and LDF are both valuable tools for assessment of cord perfusion in controlled SCI models. Acquiring high-quality, repeatable signals from such a small volume of tissue as the rat spinal cord is challenging. In particular, careful positioning of the probe is necessary; some experimentation is probably required to investigate the effect on the acquired signals of pressure applied by the probe to the tissue. An obvious technical improvement would be the fabrication of a single probe allowing simultaneous LDF and PPG measurements; e.g., by coupling a laser source (for Doppler) and LEDs (for PPG) to a single transmitting fiber, with a second fiber coupled to a photodetector suitable for both PPG and LDF modes. Multiplex/demultiplex circuitry would avoid optical interference between the two measurements. Oxygen saturation could also be calculated following the addition of a second wavelength to the PPG system.

The results presented here are promising and suggest that both PPG and LDF has the potential to yield real-time and continuous quantification of blood supply to the spinal cord tissue that may be tracked to injury events. Although LDF used individually has proved to be a useful tool for blood-flow assessment in SCI models, the addition of PPG would provide extra information regarding the integrity of the arterial supply to the region of spinal cord under investigation. Further refinements in signal processing could provide a standardized "perfusion index" that allows comparison of results from separate SCI model experiments. In addition, such a system would be useful for monitoring changes from baseline observations in the supply of blood to the tissue (e.g., during recovery from acute trauma, or following the administration of neuroprotective drugs). Optical monitoring as described in this paper will enable the continuous monitoring of perfusion in living specimens, yielding much clearer insight into the mechanisms underlying secondary ischemic injury than would be possible from postmortem examination alone. These techniques could provide powerful new tools, allowing neuroscientists to understand better the development of SCI and leading to more advanced preventative treatment strategies.

Acknowledgments

This work was supported by a grant from the *British Journal of Anaesthesia*/Royal College of Anaesthetists.

References

1. B. K. Kwon et al., "Pathophysiology and pharmacologic treatment of acute spinal cord injury," *Spine J.* **4**(4), 451–464 (2004).
2. J. W. Rowland et al., "Current status of acute spinal cord injury pathophysiology and emerging therapies, promise on the horizon," *Neurosurg. Focus* **25**(5), E2 (2008).
3. F. Castro-Moure, W. Kupsky, and H. G. Goshgarian, "Pathophysiological classification of human spinal cord ischemia," *J. Spinal Cord Med.* **20**(1), 74–87 (1997).
4. J. Y. Lee et al., "Valproic acid attenuates blood-spinal cord barrier disruption by inhibiting matrix metalloprotease-9 activity and improves functional recovery after spinal cord injury," *J. Neurochem.* **121**(5), 818–829 (2012).
5. A. P. Amar and M. L. Levy, "Pathogenesis and pharmacological strategies for mitigating secondary damage in acute spinal cord injury," *Neurosurgery* **44**(5), 1027–1039; discussion 1039–1040 (1999).
6. B. Nyström, J. E. Berglund, and E. Bergquist, "Methodological analysis of an experimental spinal cord compression model in the rat," *Acta Neurol. Scand.* **78**(6), 460–466 (1988).
7. A. Bergerot et al., "Co-treatment with riluzole and GDNF is necessary for functional recovery after ventral root avulsion injury," *Exp. Neurol.* **187**(2), 359–366 (2004).
8. D. J. Chew et al., "Segmental spinal root avulsion in the adult rat: a model to study avulsion injury induced pain," *J Neurotrauma* **30**(3), 160–172 (2012).
9. Y. P. Zhang et al., "Dural closure, cord approximation, and clot removal, enhancement of tissue sparing in a novel laceration spinal cord injury model," *J. Neurosurg.* **100**(4 Suppl Spine), 343–352 (2004).
10. R. Kurokawa et al., "Altered blood flow distribution in the rat spinal cord under chronic compression," *Spine* **36**(13), 1006–1009 (2011).
11. N. L. Martirosyan et al., "Blood supply and vascular reactivity of the spinal cord under normal and pathological conditions," *J. Neurosurg. Spine* **15**(3), 238–251 (2011).
12. V. Bartanusz et al., "Delayed post-traumatic spinal cord infarction in an adult after minor head and neck trauma, a case report," *J. Med. Case. Rep.* **6**(1), 314 (2012).
13. E. M. Nemoto, "Pathogenesis of cerebral ischemia-anoxia," *Crit. Care Med.* **6**(4), 203–214 (1978).
14. P. J. Lindsberg et al., "Validation of laser-Doppler flowmetry in measurement of spinal cord blood flow," *Am. J. Physiol.* **257**(2 Pt 2), H674–H680 (1989).
15. P. J. Lindsberg et al., "Laser-Doppler flowmetry in monitoring regulation of rapid microcirculatory changes in spinal cord," *Am. J. Physiol.* **263**(1 Pt 2), H285–H292 (1992).
16. T. Yamada et al., "Spinal cord blood flow and pathophysiological changes after transient spinal cord ischemia in cats," *Neurosurgery* **42**(3), 626–634 (1998).
17. J. L. Olive, K. K. McCully, and G. A. Dudley, "Blood flow response in individuals with incomplete spinal cord injuries," *Spinal Cord* **40**(12), 639–645 (2002).
18. H. Westergren et al., "Spinal cord blood flow changes following systemic hypothermia and spinal cord compression injury: an experimental study in the rat using Laser-Doppler flowmetry," *Spinal Cord* **39**(2), 74–84 (2001).
19. D. Zvara et al., "Spinal cord blood flow after ischemic preconditioning in a rat model of spinal cord ischemia," *ScientificWorldJournal* **4**, 892–898 (2004).
20. N. Vongsavan and B. Matthews, "Some aspects of the use of laser Doppler flow meters for recording tissue blood flow," *Exp. Physiol.* **78**(1), 1–14 (1993).
21. P. A. Oberg, "Tissue motion—a disturbance in the laser-Doppler blood flow signal?," *Technol. Health Care* **7**(2–3), 185–192 (1999).
22. D. R. Smith, H. J. Smith, and R. K. Rajjoub, "Measurement of spinal cord blood flow by the microsphere technique," *Neurosurgery* **2**(1), 27–30 (1978).
23. H. J. Senter and J. L. Venes, "Altered blood flow and secondary injury in experimental spinal cord trauma.," *J. Neurosurg.* **49**(4), 569–578 (1978).
24. C. E. Kang et al., "Spinal cord blood flow and blood vessel permeability measured by dynamic computed tomography imaging in rats after localized delivery of fibroblast growth factor," *J. Neurotrauma* **27**(11), 2041–2053 (2010).

25. J. Allen, "Photoplethysmography and its application in clinical physiological measurement," *Phys. Meas.* **28**(3), R1–R39 (2007).
26. A. W. Granelli and I. Ostman-Smith, "Noninvasive peripheral perfusion index as a possible tool for screening for critical left heart obstruction," *Acta Paediatr.* **96**(10), 1455–1459 (2007).
27. J. P. Phillips et al., "An optical fiber photoplethysmographic system for central nervous system tissue," in *Conf. Proc. IEEE Eng. Med. Biol. Soc.*, pp. 803–806, IEEE Service Center, Piscataway, New Jersey (2006).
28. J. P. Phillips et al., "Investigation of photoplethysmographic changes using a static compression model of spinal cord injury," in *Conf. Proc. IEEE Eng. Med. Biol. Soc.*, pp. 1493–1496, IEEE Service Center, Piscataway, New Jersey (2009).
29. N. E. Almond, D. P. Jones, and E. D. Cooke, "Noninvasive measurement of the human peripheral circulation, relationship between laser Doppler flowmeter, and photoplethysmograph signals from the finger," *Angiology* **39**(9), 819–829 (1988).

Biographies and photographs of the authors not available.